

EFFECT OF INDIUM DOPING ON STRUCTURAL, OPTICAL AND ELECTRICAL PROPERTIES OF CADMIUM SULFIDE THIN FILMS

R. OLVERA-RIVAS^a, F. DE MOURE-FLORES^a, S. A. MAYÉN-HERNÁNDEZ^a,
J. QUIÑONES-GALVAN^b, A. CENTENO^b, A. SOSA-DOMÍNGUEZ^a,
J. SANTOS-CRUZ^{a,*}

^a*Facultad de Química, Materiales-Energía, Universidad Autónoma de Querétaro,
C.P. 76101 Qro., México*

^b*Departamento de Física, Centro Universitario de Ciencias Exactas e Ingenierías,
Universidad de Guadalajara, Blvd. Marcelino García Barragán 1421 C.P. 44430,
Guadalajara, Jal., México*

Indium doped CdS thin films, with different In/CdS ratios, were fabricated employing chemical bath deposition technique. The incorporation of indium was carried out in the first stages of the process. The effects of In-doping on structural, surface, optical and electrical properties were determined using X-Ray Diffraction (DRX), Scanning Electron Microscope (SEM), UV-VIS Spectroscopy and Hall Measurements respectively. XRD studies showed cubic structures for all samples and that In³⁺ ions were incorporated into the lattice substitutionally at low concentration, and interstitially at high concentration. SEM measurements revealed that films morphology was unaffected by indium doping. The transmittance of In doped films was above 70% for all samples and the calculated band gap was between 2.32 and 2.44 eV. The electrical properties show an increment in carrier concentration from $1.3 \times 10^{15} \text{ cm}^{-3}$ to $2 \times 10^{16} \text{ cm}^{-3}$ and decrease in the resistivity from $2.13 \times 10^{16} \Omega$ to $1.5 \times 10^{15} \Omega$ due to indium doping.

(Received February 14, 2020; Accepted July 1, 2020)

Keywords: CdS, Chemical bath deposition, Thin films, In-doping, Solar cells,
Semiconductors

1. Introduction

Cadmium sulfide (CdS) is an II-VI semiconductor compound widely used as a window layer in thin-film solar cells based on cadmium telluride (CdTe), copper indium gallium sulfide and diselenide (CIGS or CIGSe), and copper zinc tin sulfide (CZTS) absorbers [1-3]. This is due to its excellent optical and electrical properties, such as a direct band gap energy of 2.42 eV [4,5], an absorption coefficient of $4 \times 10^4 \text{ cm}^{-1}$ [6], therefore only 100 nm thickness is required to absorb about 63% of the incident radiation [5].

There are several deposition techniques used for the deposition of CdS thin film, such as spray pyrolysis, RF sputtering, electrochemical deposition, close spaced sublimation, pulsed laser deposition and sol-gel, [1, 6-9]. It has been observed that each deposition process produces different structural, electrical and optical properties of the CdS thin films. However, one of the simpler methods to prepare CdS films at low temperature, economic, competitive results and covering large areas, almost any shape and substrate type (conductor or non-conductor) respectively, is the chemical bath deposition (CBD) [10]. A typical CdS thin films production technique by CBD starting to add Cadmium Chloride, Ammonium Nitrate, and Potassium Hydroxide after heating to a

* Corresponding author: jsantos@uaq.edu.mx

specific temperature Thiourea added to start the fabrication process [17-18]. CdS mainly exists as hexagonal or cubic phases. Currently, the highest efficiency of CdS/CdTe solar cells has already reached 22.1% [19] with the growth of CdS thin film by CBD.

On the other hand, the production of thin n-type CdS films requires extrinsic doping. Some of the most commonly used elements for doping are In, Al, Ga and B [10-12], these elements help to reduce photo decay or the dark resistivity, some studies had been reported values of 10^8 - 10^{10} Ω -cm [13-15], this resistivity values are high for optoelectronic applications as a window layer. Furthermore, it was found that indium-doped CdS thin films showed lower resistivity and better doping effect than those doped with other elements. CdS:In films were also found to be a very desirable window layer material [16].

Several chemical and physical methods have been studied for doping CdS, however, introducing indium to the lattice through a chemical bath is no trivial. In this work, CdS was effectively doped using InCl_3 . The aim of this research work is to investigate the effectiveness of In^{3+} doping through CBD, un-doped CdS samples were grown at different deposition temperatures to found optimal deposition conditions. The effect of indium doping in 0.2, 0.4, 0.6, 0.8 and 1 atomic % was studied.

2. Experimental procedure

2.1. Preparation of CdS:In films

In this research work, all the reagents used were of 99.99%, in addition they were not subjected to any purification. CdS films were grown on glass slides in a typical CBD process. The method of washing the slides was done with Extran soap, then cleaning with an acid-chromic solution and finally a chemical etching with a 10 % HNO_3 : H_2O solution.

The CBD process was carried out in a glass reactor, the previously washed glass slides used as substrate, were placed over a PTFE base vertically inside of them, then 150 ml of deionized water was added and started to heat up to 40 °C, after that the solutions of CdCl_2 (0.03M), NH_4Cl (0.075M) and Thiourea (0.05M) were added. In all the process, the solution was keeping stirred with magnetic stirring at 3 Hz.

Three different deposition temperatures were analyzed (70, 80 and 90 °C). When each final temperature was reached, 10 ml of NH_4OH was added, then InCl_3 solutions with 0.2, 0.4, 0.6, 0.8 and 1 atomic percentages were added to the reactor in each case, heating and stirring were kept constant for 1 hour. Once the reaction process of the chemical bath finished, the slides were removed from the reactor and immediately rinsed with deionized water and dried with nitrogen (N_2).

2.2. Characterization

Transmittance measurements of doped and un-doped CdS films in order to study the effect of indium doping on the optical properties and bandgap was performed using a spectrophotometer Uv-Vis Genesys 10S. The resistivity, mobility and carrier concentration of doped films were measured using Ecopia HMS-3000 Hall effect system. The crystal structure and crystal quality and phase were determined using Panalitical Empyrean X-ray diffractometer (XRD) with $\text{Cu } \alpha$ radiation ($\lambda = 1.5406 \text{ \AA}$) and Thermo Scientific DRX2 Raman spectrometer with 532 nm laser wavelength. The surface morphology and stoichiometry of the films was studied by means of scanning electron microscope (SEM) with 20 kV electron high tension and energy dispersive X-ray (EDX) using Tescan Mira 3 FEG-SEM instrument. A KLA Tecnor D-100 surface profilometer was used to determine film thicknesses.

3. Results and discussion

3.1. Optical properties

The transmittance spectra of CdS:In thin films were measured to study the effect of temperature and indium concentration on the optical properties of CdS thin films which is shown in Fig. 1. It shows the optical transmittance spectra for wavelengths ranging from 300 to 1000 nm. Fig.1 a) corresponds to un-doped films produced with different process temperature and Fig.1. b) shows spectra for doped CdS thin films at a constant temperature of 90° C and varying the indium concentration.

The transmittances of almost all films are higher than 70%, desirable for its use as a window film; however, it can be observed when the In dopants were added, the average transmittances in the visible region increased. The reason for this happening it can be explained when the In is added to the CdS, only the growth of CdS crystallization was moderate to form a smoother surface and that surface improved optical transmittance by reducing optical dispersion. [20-21].

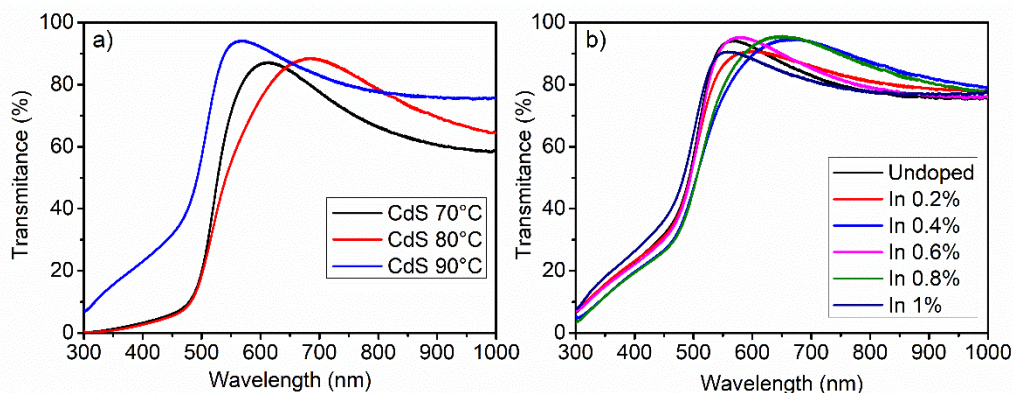


Fig. 1. UV-Visible transmittance spectra of a) CdS films and b) In doped CdS thin films.

It is well known that CdS thin films have direct transitions. The optical energy band gap E_g can be calculated according to Tauc model [22, 23]:

$$\alpha h\nu = A(h\nu - E_g)^{1/2} \quad (1)$$

where α is the absorption coefficient, h is Planck's constant, A is a constant and E_g is the band gap, respectively. E_g can be obtained through extrapolating $(\alpha h\nu)^2$ vs. photon energy ($h\nu$). The band gaps were found to be in the range 2.32 eV – 2.44 eV as shown in Fig 2. When the indium concentration continues increasing to a higher value of 1%, the band gap increases with indium concentration except by 0.8%. The effect of widening of the optical band gap with indium doping can be described by Burstein-Moss effect [24, 25]. The Burstein-Moss effect is presented because of the carrier contribution from the In^{3+} ions on substitutional sites of Cd^{2+} ions. Additionally, indium interstitial atoms increase the carrier concentration, and the band gap of the doped material is increased due to the Fermi level moving into the conduction band.

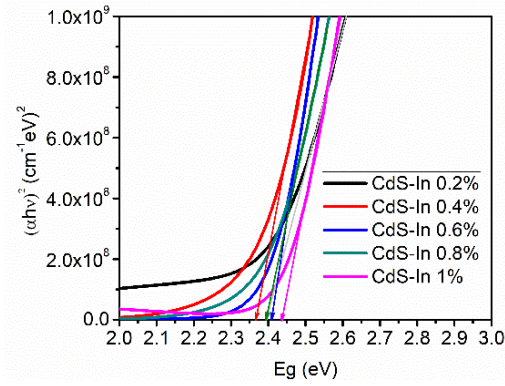


Fig. 1. The band gap of CdS films vs. indium concentration.

3.2. Structural properties

The samples prepared by CBD presented a uniform green-yellowish color, transparent and of good adherence to the substrate. The XRD patterns of the un-doped and doped CdS thin films are shown in Fig. 3. In all samples only one peak at $2\theta = 26.45^\circ$ which corresponds to (111) plane of cubic CdS (PDF #65-2887) appears. Cubic CdS is metastable phase at room temperature. Thermal annealing was not applied to the samples therefore hexagonal phase is discarded.

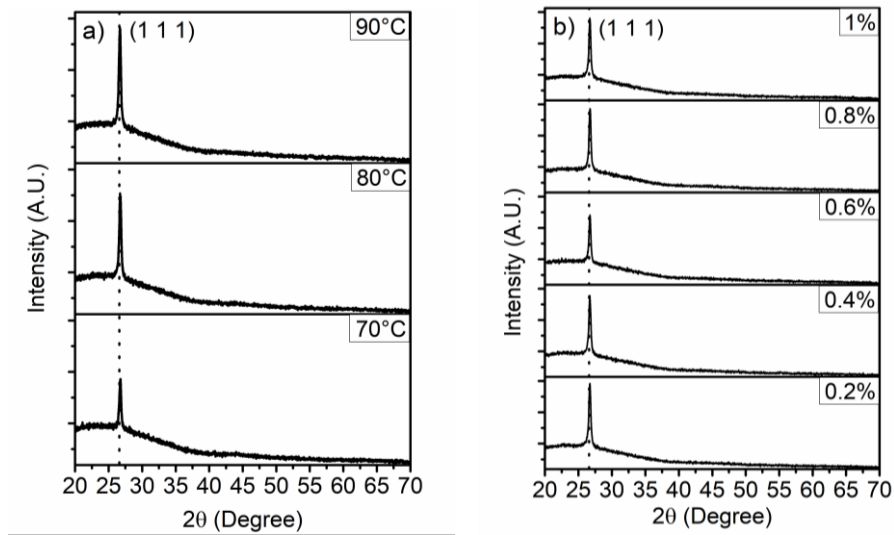


Fig. 3. XRD pattern of a) CdS un-doped films at different temperature and b) indium-doped CdS films.

As shown in Fig. 3 b), no peaks of In, In_2S_3 , were detected, which indicates that incorporation of In^{3+} ions does not form secondary compounds like In_2S_3 . The average (1 1 1) interplanar distance $d_{(111)}$ was calculated using the formula:

$$n\lambda = 2d \sin(\theta) \quad (2)$$

where λ is the X-ray wavelength (1.5406 Å), and θ is the Bragg angle. Crystallite size was calculated using the Debye-Scherrer formula:

$$D = \frac{0.9\lambda}{\beta \cos \theta} \quad (3)$$

where β is the full width at half maximum (FWHM) of the preferential peak and θ is the Bragg angle. As shown in Fig. 4, as the % of indium increases, the spacing of the (1 1 1) lattice planes decreases below that of un-doped films until it reaches a minimum in 0.6 at %, then, for in 1 at. % increases. Considering that the ionic radius In^{3+} (0.81 Å) is smaller than that of Cd^{2+} (0.97 Å) [26], it is suggested that the In^{3+} ions replace Cd^{2+} ions in the lattice substitutionally, which results in smaller $d_{(1\ 1\ 1)}$ values than that of undoped CdS film. However, the interplanar distance is maintained at 0.6 at. %. At this concentration the In^{3+} ions starts to entering into the lattice both substitutionally and interstitially which caused the $d_{(1\ 1\ 1)}$ values to increase again and that is observed for the 1% concentration there is an increase in the distance.

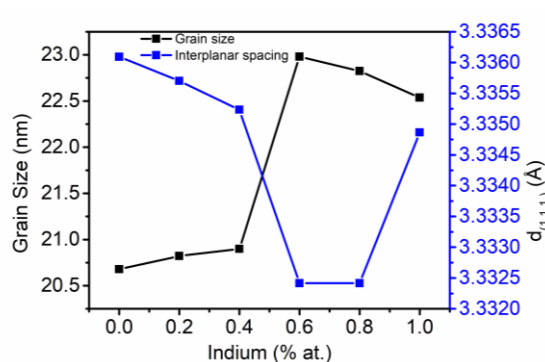


Fig. 4. Interplanar distance $d_{(1\ 1\ 1)}$ and grain size relation as a function of indium at. %.

On the other hand, it can be observed that the crystallite size increases with increasing indium concentration, and then when the indium is of 0.6%, the crystallite size starts to decrease. This decrease in crystallite size could cause lattice strain by the incorporation of the indium substitutionally and interstitially as a compression or tension stress.

The Raman analysis results for doped films are shown in Fig 5. The Raman spectra of doped CdS films shown a vibrational asymmetric modes and a well-resolved line at approximately $290\ \text{cm}^{-1}$, corresponding to the first order scattering of the longitudinal optical (LO) phonon mode for CdS. The second-order scattering of LO phonon is also visible at approximately $6588\ \text{cm}^{-1}$. It can be seen the asymmetric signal of 1LO increases as the indium percentage also increases, this is due to the effect of stress induced by the incorporation of the indium into the crystalline lattice in addition to the result of the high density of stacking faults during growth processes in CBD reactor [27].

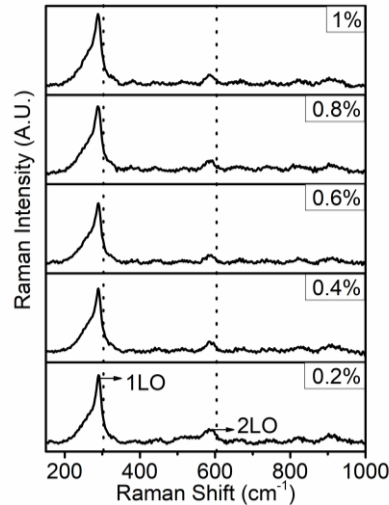


Fig. 5. Raman Spectra of indium doped CdS thin films.

3.3. Electrical properties

Hall measurements were performed to determine the electrical properties as a function of indium content. Results are shown in Fig. 6. The carrier concentration (CC) in black square, for undoped film it has the lowest CC, about $1.3 \times 10^{15} \text{ cm}^{-3}$ and as the indium content increases in the film, the CC also increases up to a maximum of $2 \times 10^{16} \text{ cm}^{-3}$. Regarding resistivity blue triangle, as the indium content of increases, the resistivity decreases. This is attributed to the increase of extra electrons for the In^{3+} ions which replaced the Cd^{2+} sites and reduced the potential barrier of CdS grain boundary [19], however at 0.6% a slight increase in the resistivity is seen because, as mentioned above, the ions begin to enter in the lattice both substitutionally and interstitially. Interstitial In^{3+} ions will act as recombination centers decreasing the CC and increasing the resistivity [28]. The mobility (red circle), as a result of increment of CC also increases as indium is incorporated.

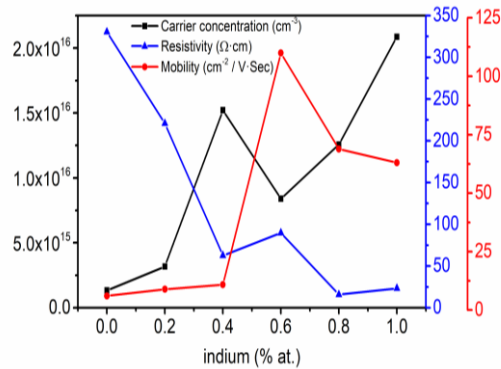


Fig. 6. Variation of carrier concentration, resistivity and mobility versus indium concentration.

3.4. Morphological analysis

Fig. 7 shows the SEM images for doped and un-doped CdS. All the films have a thickness between 120 nm – 150 nm. The images show a large density of smaller grains and a small density

of large grains in all cases, this indicates that indium doping did not have a significant effect on the morphology of CdS film, all films are smooth, continuous and uniform.

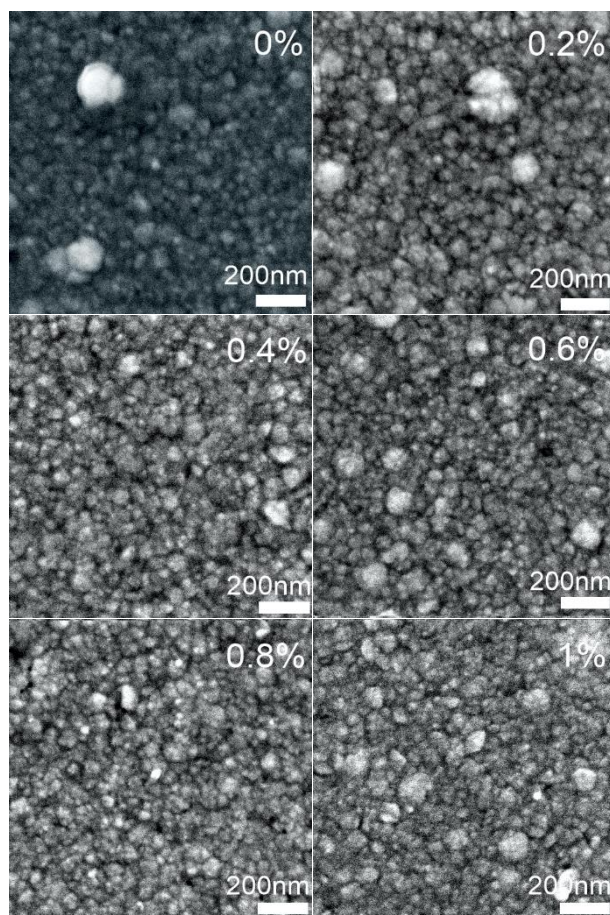


Fig. 7. SEM images for CdS doped and undoped films.

4. Conclusions

CdS thin films were deposited on glass substrates by CBD technique. The films were successfully doped with indium during the first steps of growth at temperature of 90°C. All doped films exhibit high transmittance (upper 80%). X-Ray diffraction and Raman spectroscopy, confirmed that the CdS:In thin films are crystalline in the cubic phase which is a metastable phase. Doping does not affect the crystalline structure of the films. A resistivity as low as 15.83 Ω cm and a carrier concentration as high as $2 \times 10^{16} \text{ cm}^{-3}$ have been achieved for a 1% of atomic concentration of indium.

In the analysis of interplanar distances and grain sizes, the influence of the incorporation of In^{3+} ions are observed for atomic concentration values lower than 0.6 at. % in which replacement of Cd^{2+} ions for In^{3+} is substitutional. For higher indium nominal content values, indium In^{3+} ions incorporation into the lattice is both substitutional and interstitial. SEM analysis showed that doping did not affect the morphology of all the films. Finally, the calculated band gap values are around 2.32 – 2.4 eV confirming that the films are potential candidates for solar cell applications.

5. References

- [1] N. A. Shah, R. R. Sagar, W. Mahmood, W. A. A. Syed, *J. Alloys Compd.* **512**(1), 185 (2012).
- [2] F. Lisco et al., *Thin Solid Films* **582**, 323 (2015).
- [3] D. M. Meysing et al., *J. Vac. Sci. Technol. Vac. Surf. Films* **33**(2), 021203 (2015).
- [4] M. F. Saleem, H. Zhang, Y. Deng, D. Wang, *J. Raman Spectrosc.* **48**(2), 224 (2017).
- [5] T. L. Chu, S. S. Chu, *Prog. Photovolt. Res. Appl.* **1**(1), 31 (1993).
- [6] B. Altiokka, A. K. Yildirim, *J. Korean Phys. Soc.* **72**(6), 687 (2018).
- [7] *Int. J. Mater. Chem.*, p. 5, 2018.
- [8] G. Perna et al., *Thin Solid Films* **453-454**, 187 (2004).
- [9] B. Su, K. L. Choy, *Thin Solid Films*, p. 5, 2000.
- [10] H. Khallaf, G. Chai, O. Lupan, L. Chow, S. Park, A. Schulte, *J. Phys. Appl. Phys.* **41**(18), 185304 (2008).
- [11] A. Fatehmulla, A. S. Al-Shammari, A. M. Al-Dhafiri, W. A. Farooq, F. Yakuphanoglu, Structural, Electrical and Optical Properties of Chlorine Doped CdS Thin Films, p. 7, 2014.
- [12] B. Ghosh, K. Kumar, B. K. Singh, P. Banerjee, S. Das, *Appl. Surf. Sci.* **320**, 309 (2014).
- [13] C. GuilleÅn, M. A. MartÅñez, J. Herrero, *Thin Solid Films*, p. 6, 1998.
- [14] M. T. S. Nair, P. K. Nair, J. Campos, *Thin Solid Films* **161**, 21 (1988).
- [15] O. Vigil, O. Zelaya-Angel, Y. Rodriguez, *Semicond. Sci. Technol.* **15**(3), 259 (2000).
- [16] M. A. Islam et al., «Opto-electrical properties of in doped CdS thin films by co-sputtering technique», p. 6.
- [17] H. C. Chou, A. Rohatgi, E. W. Thomas, S. Kamra, A. K. Bhat, *J. Electrochem. Soc.* **142**(1), 254 (1995).
- [18] M. Potter, M. Cousins, K. Durose, D. P. Halliday, *J. Mater. Sci. Mater. Electron.* **11**, 525 (2000).
- [19] Y. Chen et al., *Chalcogenide Lett.* **14**(1), 2017.
- [20] J.-H. Lee, B.-O. Park, *Thin Solid Films* **426**(1), 94 (2003).
- [21] C. Y. Tsay, H. C. Cheng, Y. T. Tung, W. H. Tuan, C. K. Lin, *Thin Solid Films* **517**(3), 1032 (2008).
- [22] P. Praus, O. Kozák, K. Kočí, A. Panáček, y R. Dvorský, *J. Colloid Interface Sci.* **360**(2), 574 (2011).
- [23] M. A. Hossain et al., *J. Mater. Chem.* **22**(32), 16235 (2012).
- [24] T. S. Moss, *Proc. Phys. Soc. Sect. B* **67**(10), 775 (1954).
- [25] R. Cebulla, R. Wendt, K. Ellmer, *J. Appl. Phys.* **83**(2), 1087 (1998).
- [26] J. E. Huheey, *Inorganic chemistry: principles of structure and reactivity*, New York, Cambridge, Philadelphia etc., Harper and Row Publishers, 1983.
- [27] I. Oladeji et al., *Thin Solid Films* **359**(2), 154 (2000).
- [28] J. A. Akintunde, *J. Mater. Sci. Mater. Electron.* **11**(6), 503 (2000).